

Network Planning Strategies for Next-Generation Flexible Optical Networks [Invited]

Original

Network Planning Strategies for Next-Generation Flexible Optical Networks [Invited] / Rosanna, Pastorelli; Bosco, Gabriella; Stefano, Piciaccia; Fabrizio, Forghieri. - In: JOURNAL OF OPTICAL COMMUNICATIONS AND NETWORKING. - ISSN 1943-0620. - STAMPA. - 7:3(2015), pp. A511-A525. [10.1364/JOCN.7.00A511]

Availability:

This version is available at: 11583/2603593 since: 2016-08-03T13:06:42Z

Publisher:

OSA Optical Society of America

Published

DOI:10.1364/JOCN.7.00A511

Terms of use:

This article is made available under terms and conditions as specified in the corresponding bibliographic description in the repository

Publisher copyright

Optica Publishing Group (formely OSA) postprint/Author's Accepted Manuscript

“© 2015 Optica Publishing Group. One print or electronic copy may be made for personal use only. Systematic reproduction and distribution, duplication of any material in this paper for a fee or for commercial purposes, or modifications of the content of this paper are prohibited.”

(Article begins on next page)

Network Planning Strategies for Next-Generation Flexible Optical Networks [Invited]

Rosanna Pastorelli, Gabriella Bosco, *Senior Member, IEEE*, Stefano Piciaccia and Fabrizio Forghieri, *Member, IEEE*

Abstract— Using well-established results on non-linear propagation modeling in coherent optical links, two different approaches for network planning are addressed and compared in terms of performance maximization and robustness to dynamic changes in the network, one based on the maximization of the margin in optical signal-to-noise-ratio (OSNR), the other on the minimization of the pre-FEC bit error rate (BER). We show that, in pure coherent optical networks, the planning strategy that best supports the dynamic evolution of the network is the design aimed at BER minimization. A closed-form formula for the maximum reach (in terms of number of spans and loss budget) of each interface is analytically derived, which is a useful tool for the evaluation of the overall network cost for a desired traffic capacity.

Index Terms— Optical fiber networks, network optimization, coherent communications, GN-model.

I. INTRODUCTION

Next generation optical networks will be characterized by the use of coherent optical detection, the absence of optical dispersion management and a large variety of symbol-rates, channel spacings and modulation formats [1]. As a consequence, network design and planning operations for such networks will be based not only on a criterion of cost minimization but they will also require a maximization of the “flexibility”. The operative conditions of coherent channels in the network can have a significant role on how optical traffic can be dynamically changed over time and, consequently, channel settings configurations impact the network planning flexibility.

Specifically, next generation optical networks will have to support both a dynamic evolution of the transport layer with the changes of traffic volumes (long-term variations with no “a-priori” knowledge of the future traffic matrix) or

the modification of traffic optical paths (short-term variations, consequence, for example, of restoration events involving the physical layer) and the management of physical layer maintenance operations in the system evolution from beginning-of-life (BOL) to end-of-life (EOL).

In this work we resort to a well-established and computationally efficient analytical physical model for non-linear propagation in uncompensated optical systems with coherent detection, known as the “GN-model” [2], in order to identify the best way to support network planning strategy in terms of traffic performance maximization and robustness to (short and long term) dynamic changes in the network. We extend here the preliminary analysis reported in [3], analyzing more in depth the network planning strategies and providing additional case studies which give a better insight to the characteristics of the two analyzed methodologies.

In Section II, we introduce the relevant features of the GN-model, showing how it can be used to predict the performance of an optical link in terms of pre-FEC (forward error correction) BER (bit error rate) vs. the optical signal-to-noise ratio (OSNR) at the input of the receiver. Section III is then devoted to the description of the two alternative network planning strategies, based on the optimization of the launched power for maximization of either the OSNR margin or the BER margin, respectively. In Section IV some case studies are analyzed in order to compare the performance of the two alternative network planning strategies, assessing the sensitivity of the system performance to the variation of network characteristics, such as traffic matrix, transponders, amplifiers and fiber. In Section V a global analytical formula is reported which highlights the scaling of the maximum achievable length of the link with the systems parameters (i.e. transponder performance and amplification layer characteristics). We propose the derived formula as a useful tool for the estimation of the network costs. Finally, in Section VI some conclusions are drawn.

II. FIBER PROPAGATION MODEL

The GN-model [2] provides a simple analytical tool that can be used to accurately predict the performance of an optical uncompensated point-to-point link. The two basic assumptions of the GN-model, which are in common to other perturbation models of nonlinear propagation in

Manuscript received June 30, 2014. R. Pastorelli, S. Piciaccia and F. Forghieri are with Cisco Photonics Italy srl, 20871 Vimercate, Italy (rpastore@cisco.com). G. Bosco is with the Electronic and Telecommunication Department, Politecnico di Torino, 10129, Torino, Italy (gabriella.bosco@polito.it).

uncompensated optical fiber systems [4]-[7], are:

- Both linear and non-linear (NL) effects can be treated as two independent and uncorrelated additive noise components.
- The total “equivalent” optical signal-to-noise ratio (OSNR) at the end of an optical link can be written as:

$$\text{OSNR}_{\text{TOT}} = \frac{P_{Tx}}{P_{ASE} + P_{NLI}} = \left(\frac{1}{\text{OSNR}_{ASE}} + \frac{1}{\text{OSNR}_{NL}} \right)^{-1} \quad (1)$$

P_{Tx} is the power per channel at the input of each fiber span, P_{ASE} and P_{NLI} are, respectively, the power of the noise introduced by the optical amplifiers and the power of the non-linear interference, both evaluated over a bandwidth equal to B_n . $\text{OSNR}_{ASE} = P_{Tx}/P_{ASE}$ and $\text{OSNR}_{NL} = P_{Tx}/P_{NLI}$, are the linear and non-linear OSNR, respectively (the main symbols used throughout the paper are listed in Table I, together with their definitions). EDFA's are considered to work in constant-gain mode: whenever the equal span length assumption is used, EDFA gain and noise working points can be fairly assumed to be constant when total signal power in fiber is changed.

In case of a multi-span link composed of N_{span} fiber spans, P_{ASE} and P_{NLI} can be written as:

$$P_{ASE} \cong B_n h \nu \sum_{k=1}^{N_{span}} F^{(k)} A_{span}^{(k)}, \quad P_{NLI} \cong B_n \sum_{k=1}^{N_{span}} \eta^{(k)} \left(P_{Tx} \right)^3 \quad (2)$$

where $F^{(k)}$ is the noise figure of the k -th optical amplifiers, $A_{span}^{(k)}$ is the loss of the k -th fiber span (in linear units), h is the Plank's constant, ν is the center propagation frequency and $\eta^{(k)}$ is the non-linearity coefficient of the k -th span, which depends on the fiber characteristics (local chromatic dispersion, refractive index, effective area, attenuation coefficient and length) and on the traffic matrix (i.e., number of transmitted channels, spacing between them, channel spectral shape and bandwidth) [2]. In case of a homogeneous multi-span link composed of N_{span} identical fiber spans, each with a total loss equal to A_{span} and characterized by the same nonlinearity coefficient η , using the incoherent GN model [2] which assumes that the non-linear noise generated in each span adds up incoherently, Eq. (2) can be simplified to:

$$P_{ASE} \cong N_{span} h \nu F A_{span} B_n, \quad P_{NLI} \cong N_{span} \eta P_{Tx}^3 B_n \quad (3)$$

A generic transponder (TXP) is characterized by a back-to-back (btb) performance, which can be expressed as a function of the linear OSNR, as:

$$\text{BER}_{\text{btb}} = \Phi(\text{OSNR}_{ASE}) \quad (4)$$

where the expression of Φ depends on the modulation formats and TXP characteristics and BER is the pre-FEC bit error rate (i.e. before FEC decoding). As an example, for an ideal TXP employing a dual Coherent-Polarization DQPSK modulation (CP-DQPSK):

$$\text{BER}_{\text{btb}} \approx \text{erfc} \left(\sqrt{\frac{B_n \text{OSNR}_{ASE}}{R_s}} \right) \quad (5)$$

where R_s is the symbol rate.

An example of btb curve for a 100Gb/s CP-DQPSK transponder is shown in Fig. 1 (grey curve). The red horizontal straight line indicates the FEC threshold, set to $\text{BER}_{\text{FEC}} = 4 \cdot 10^{-3}$. The black curve shows the performance of the TXP after propagation considering only the impact of

linear propagation effect, e.g., polarization dependent loss (PDL), polarization mode dispersion (PMD) and chromatic dispersion (CD) compensation impairments, linear cross-talk impairments of the system, when present, etc. The sources and the impact of these linear effects in the BER degradation with respect to btb depend on both transmission system and TXP characteristics; whatever is the amount of linear propagation impairments, the linear performance of the considered TXP in the selected transmission scenario allows the definition of the OSNR_{FEC} as the OSNR at FEC correction threshold in the linear propagation regime.

Using the GN-model, it is possible to generate BER vs. OSNR_{ASE} curves in NL propagation regime by evaluating the NL effects at different values of the launched power P_{Tx} . The solid green curve shows an example of such evolution for a fixed value of P_{Tx} in the described transmission scenario. Note that, once P_{Tx} is selected, the linear OSNR at the receiver, $\text{OSNR}_{ASE,Rx}$, and the corresponding non-linear OSNR, OSNR_{NL} , are determined, through Eqs. (1) and (2).

TABLE I
LIST OF SYMBOLS

Symbol	Definition
N_{span}	Number of spans
A_{span}	Span loss
F	Amplifier noise figure [dB]
B_n	Noise reference bandwidth [Hz]
η	Non-linearity coefficient [Hz/W ²]
P_{Tx}	Fiber launched power [W]
P_{NLI}	Power of non-linear interference [W]: $N_{span} \eta P_{Tx}^3 B_n$
P_{ASE}	Total power of ASE noise [W] (including noise loading)
$P_{ASE,Rx}$	Power of ASE noise at the end of the transmission link [W]: $N_{span} h \nu F A_{span} B_n$
OSNR_{ASE}	Linear OSNR: P_{Tx}/P_{ASE}
OSNR_{NL}	Non-linear OSNR: P_{Tx}/P_{NLI}
OSNR_{TOT}	Total OSNR (including both linear and non-linear contributions): $\frac{P_{Tx}}{P_{ASE} + P_{NLI}}$
OSNR_{FEC}	OSNR_{ASE} at FEC BER threshold in linear propagation regime
$\text{OSNR}_{\text{FEC,NL}}$	OSNR_{ASE} at FEC BER threshold in non-linear propagation regime
$\text{OSNR}_{ASE,Rx}$	Linear OSNR at the Rx (without noise loading): $P_{Tx}/P_{ASE,Rx}$
$\text{OSNR}_{\text{margin}}$	$\text{OSNR}_{ASE,Rx} / \text{OSNR}_{\text{FEC,NL}}$
$\text{BER}_{\text{margin}}$	Difference between the pre-FEC BER at the system working point and the pre-FEC BER at FEC correction threshold (see Fig.2)
$\text{OSNR}_{NL,pen}$	At a fixed BER, horizontal distance between the non-linear (green) and the linear (black) curve in Fig. 2: $\text{OSNR}_{ASE} / \text{OSNR}_{\text{TOT}}$
$\text{BER}_{NL,penalty}$	At a fixed OSNR_{ASE} , vertical distance between the non-linear (green) and the linear (black) curve in Fig. 2

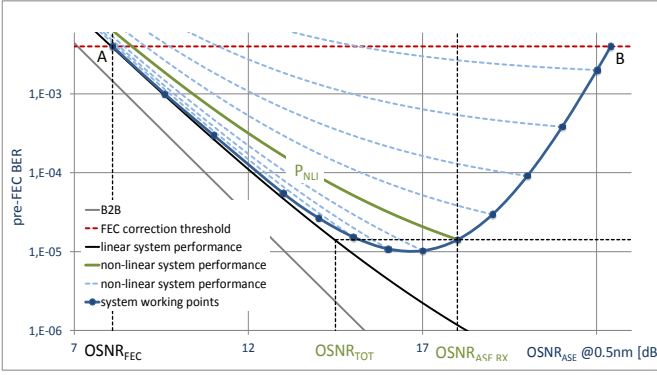


Fig. 1. Evolution of pre-FEC BER vs. $OSNR_{ASE}$ (see text for details). The reference system is composed of 5 uncompensated spans of standard single mode fiber (SSMF with $\alpha=0.22\text{dB/km}$; $CD=16.7\text{ps/nm/km}$) with loss 22dB with 80x100Gb/s CP-DQPSK WDM (wavelength division multiplexing) signal at 50 GHz spacing. The labels $OSNR_{ASE,RX}$ and $OSNR_{TOT}$ below the x-axis are referred to the solid green line (i.e. correspond to a particular value of P_{Tx}): they indicate the values of linear OSNR at the receiver (without noise-loading) and total OSNR, respectively.

This allows the estimation of the $OSNR_{tot}$, which is related to the pre-FEC BER at P_{Tx} through the linear performance curve (black solid line in Fig. 1). This approach can be extended for different values of P_{Tx} : for each value of P_{Tx} , it is possible to estimate the total power of noise affecting the transmitted signal, as the sum of the non-linear noise P_{NLI} and the ASE noise P_{ASE} . Each light blue curve in Fig. 1 shows the evolution of the pre-FEC BER vs. $OSNR_{ASE}$, obtained by keeping the launched power constant (i.e. keeping P_{NLI} fixed) and decreasing the TXP performance by means of ASE noise loading at the receiver side. Conversely, changing the fiber launched power, both the non-linear noise P_{NLI} and the value of $OSNR_{ASE}$ without noise loading (indicated as $OSNR_{ASE,RX}$) change: accordingly, the dependence of BER performance on $OSNR_{ASE,RX}$ is shown by the blue curve of Fig. 1 that represents the locus of possible working points for the transmitted signal through the considered transmission system. Each point of the blue line corresponds to a specific P_{Tx} and P_{NLI} value.

If P_{Tx} is small, the impact of P_{NLI} is negligible and the light blue curves are superimposed to the black one. This region is characterized by a low value of $OSNR_{ASE,RX}$, which causes a BER increase; at the limit operational condition, BER equals the FEC correction threshold (point “A” in Fig.1). When P_{Tx} increases, $OSNR_{ASE,RX}$ improves but simultaneously the nonlinear effects and the value of P_{NLI} increase, as well, and the light blue curves in Fig. 1 move away from the linear performance. Despite the $OSNR_{ASE,RX}$ increase, the faster increment of P_{NLI} starts causing BER degradation: power increase is allowed until the signal performance reaches the FEC correction limit (point “B” in Fig.1).

In conclusion, the operative region described by the blue curve is fully spanned by varying the fiber launched power from a minimum value corresponding to the linear transmission regime limit (point A) to a maximum value corresponding to the non-linear transmission regime limit

(point B). The values of P_{Tx} corresponding to the points A and B in Fig. 1 can be found by solving in P_{Tx} the equation $OSNR_{TOT}=OSNR_{FEC}$ and, for a system with identical spans, are approximately equal to:

$$P_{opt}^A \cong OSNR_{FEC} N_{span} \cdot h\nu F A_{span} B_n \quad (6)$$

$$P_{opt}^B \cong \sqrt{\frac{1}{OSNR_{FEC} N_{span} \cdot \eta B_n}}$$

Eq. (6) reports the minimum and maximum values of launched power which guarantee a BER performance below the FEC threshold, which correspond to the boundaries of the feasibility region and thus cannot be used for the network planning. In particular, the network planning requires the identification of the working point in the blue curve that maximizes the network design flexibility and minimizes cost. We studied and proposed two alternative approaches, detailed in the following section.

III. NETWORK PLANNING STRATEGIES

In this section we derive the optimum working points, identified by the value of launched power P_{Tx} , or, equivalently, of the non-linear OSNR ($OSNR_{NLI}$), when either of the following two design strategies (detailed in the following) is used:

- Maximization of the OSNR margin of the system – see Section III.A.
- Maximization of BER margin (or, equivalently, minimization of pre-FEC BER) – see Section III.B.

Subsection III.C is then devoted to the assessment of the sensitivity of OSNR and BER margin to fiber launched power variations around the optimum.

A. Maximization of the OSNR margin of the system

The OSNR margin, in dB unit, is defined as: $OSNR_{margin} = OSNR_{ASE,RX} - OSNR_{FEC-NL}$ (see Fig.2 and Table I), where $OSNR_{FEC-NL}$ is the OSNR at FEC correction limit in the NL propagation regime and depends on the launched power. This optimization strategy is suitable for managing $OSNR_{ASE,RX}$ variations in the operative life of the network.

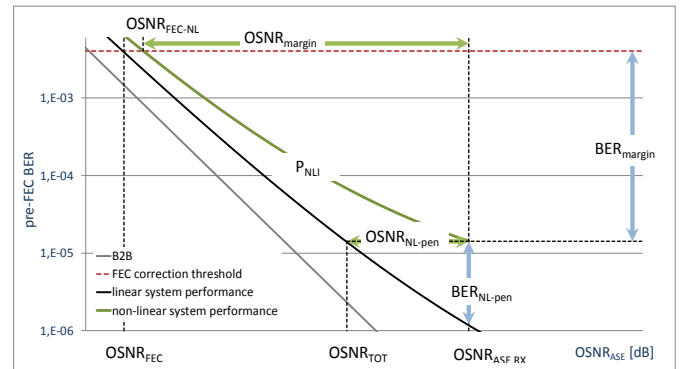


Fig. 2. Evolution of pre-FEC BER vs. $OSNR_{ASE}$, with definitions of margins and penalties (see Table I for symbols description).

As shown in Appendix A, the maximization of $OSNR_{margin}$ is achieved when working at the optimum value of $OSNR_{NLI}$, which turns out to be independent of fiber parameters and

number of spans:

$$OSNR_{NL,opt} = 3 \cdot OSNR_{FEC} \quad (7)$$

Defining the non-linear OSNR penalty ($OSNR_{NL,pen}$) as the ratio between the $OSNR_{ASE}$ and the corresponding $OSNR_{TOT}$, i.e. the distance in dB, at a fixed BER, between the non-linear (green) and the linear (black) curve in Fig. 2, it can be shown that, regardless of the working point, the value of $OSNR_{NL,pen}$ at the FEC correction limit is always equal to 2/3 (1.8 dB). The derivation of this result is shown in Appendix C.

In case of homogenous systems (equal span loss, span type and amplifier type), the optimum power P_{opt}^M corresponding to the $OSNR_{NL,opt}$ of Eq. (7) is:

$$P_{opt}^M = \sqrt{\frac{1}{3 \cdot OSNR_{FEC} N_{span} \cdot \eta B_n}} \quad (8)$$

P_{opt}^M is independent of the span loss and the EDFAs noise figure. It does depend on number of spans, on the fiber parameters and on TXP type: this means that planning at maximum OSNR margin is a *global* optimization of the link performance. In case of traffic matrix with channels that are partially in overlap (i.e., colored circuits that have different optical paths but have a subset of common spans they pass through) or that are based on TXP's having different btb performance at the FEC correction limit, each link can require a different optimum power so that the overall network optimization has to be performed using global optimization criteria. In this scenario, global optimization will necessarily result into sub-optimization of some specific links as a consequence of the need of simultaneously trying to maximize the performance of all the channels of the network.

B. Maximization of BER margin

The BER margin is defined as the difference between the pre-FEC BER at the system working point and the pre-FEC BER at FEC correction threshold (see Fig.2). This optimization strategy is suitable for managing TXP performance differences and meshed traffic matrix.

The maximization of BER margin is equivalent to the minimization of the pre-FEC BER or, equivalently, to the maximization of the Q value (with BER and Q related by the formula $BER = 0.5 \cdot \text{erfc}(Q/\sqrt{2})$). Both imply the maximization of $OSNR_{TOT}$ in Eq. (1), which, as shown in Appendix B, yields the optimum power:

$$P_{opt}^m = \sqrt[3]{\frac{h\nu FA_{span}}{2 \cdot \eta}} \quad (9)$$

For sake of clarity, in the following the strategy of BER margin maximization will be indicated as *minimum BER planning strategy*. The non-linear OSNR penalty at the minimum BER working point is the ratio between the $OSNR_{ASE,Rx}$ and the corresponding $OSNR_{TOT}$: it can be shown that this penalty is always equal to 2/3 (1.8 dB). The derivation of this result is shown in Appendix C.

In case of homogenous systems (equal span loss, span type and amplifier type), the optimum value of non-linear OSNR, corresponding to optimum power of Eq. (9) is:

$$OSNR_{NL,opt}^m = \frac{1}{N_{span} B_n} \sqrt[3]{\frac{4}{(h\nu FA_{span})^2 \eta}} \quad (10)$$

while, at the optimum, P_{ASE} and P_{NL} satisfy the condition:

$$P_{ASE}^{opt} = h\nu B_n FA_{span} = 2P_{NL}^{opt} = 2\eta B_n (P_{opt}^m)^3 \quad (11)$$

P_{opt}^m is independent of TXP type and number of spans. At span level, it does depend on the fiber parameters, the span loss and the EDFAs characteristics. It is a span-per-span local optimization of the link performance [8] and does not require a global optimization of the network based on the actual traffic matrix.

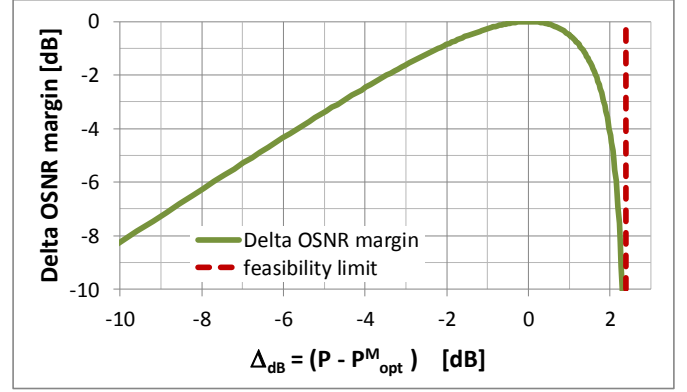


Fig. 3. Maximum OSNR margin strategy: OSNR margin penalty as a function of the launched power variation around the optimum value (Eq. (12)).

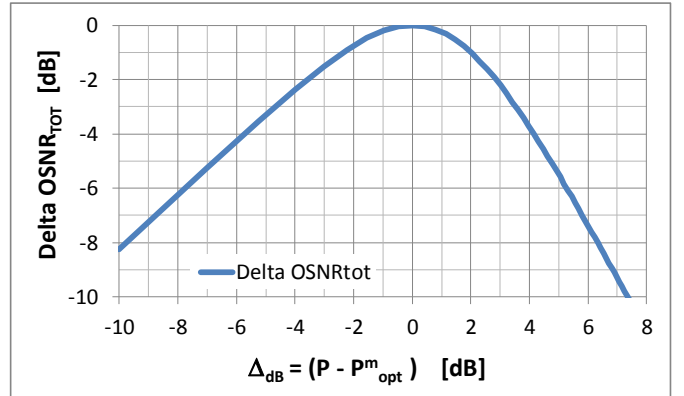


Fig. 4. Minimum BER strategy: total OSNR penalty as a function of the launched power variation around the optimum value (Eq. (13)).

C. Sensitivity to power variations around the optimum

In this section, we assess the sensitivity of OSNR margin and BER margin (expressed in terms of $OSNR_{TOT}$) to variations of the launched power around the optimum values of Eqs. (8) and (9), respectively. In order to do so, we assume that the launched power is equal to $P_{\Delta} = \Delta \cdot P_{opt}$, where P_{opt} is evaluated using either Eq. (8) or (9) in case of maximum OSNR margin strategy or minimum BER strategy, respectively. The ratio between the OSNR margin at P_{Δ} and the OSNR margin at P_{opt}^M is equal to (see

Appendix D):

$$\frac{OSNR_{\text{margin}}(P_{\Delta})}{OSNR_{\text{margin}}(P_{\text{opt}}^M)} = \frac{\Delta(3 - \Delta^2)}{2} \quad (12)$$

The OSNR margin penalty of Eq. (12) as a function of Δ in dB is plotted in Fig. 3. When $\Delta_{\text{dB}} < \sim 3\text{dB}$, the OSNR margin scales dB per dB with the power variation (this corresponds to the linear transmission regime). The margin reduction rapidly increases for $\Delta > 0$: a vertical asymptote is present when $\Delta_{\text{dB}} = 2.38\text{dB}$. In case of $\Delta_{\text{dB}} > 2.38\text{dB}$ (i.e. $\Delta^2 > 3$), the link is not feasible, regardless of the received OSNR. This behavior can be explained by the fact that $\Delta^2=3$ means $OSNR_{\text{NL}}=3 \cdot OSNR_{\text{NL,opt}}$ or, in other terms, the value of $OSNR_{\text{NL}}$ is equal to the minimum acceptable OSNR at the FEC correction limit in linear transmission conditions.

Furthermore, when $\Delta^2 > 3$ the BER vs. OSNR curves have a floor at BER values greater than the FEC correction threshold.

Similarly, in case of minimum BER strategy, the ratio between the $OSNR_{\text{TOT}}$ at P_{Δ} and the $OSNR_{\text{TOT}}$ at P_{opt}^m is equal to (see Appendix D):

$$\frac{OSNR_{\text{TOT}}(P_{\Delta})}{OSNR_{\text{TOT}}(P_{\text{opt}}^m)} = \frac{3\Delta}{(2 + \Delta^3)} \quad (13)$$

The OSNR margin penalty of Eq. (13) as a function of Δ in dB is plotted in Fig. 4. When $\Delta_{\text{dB}} < \sim 3\text{dB}$ the $OSNR_{\text{TOT}}$ penalty scales dB per dB with the power variation (this corresponds to the linear transmission regime). Small power variations around the optimum power result into small equivalent OSNR margin variations: $\Delta P = \pm 1$ dB corresponds to $\Delta OSNR_{\text{tot}} = -0.21/-0.24\text{dB}$, whilst $\Delta P = \pm 2$ dB corresponds to $\Delta OSNR_{\text{tot}} = -0.75/-1.0$ dB. The $OSNR_{\text{TOT}}$ penalty increases faster when $\Delta > 1$, i.e. in the non-linear regime. Note that, depending on the card FEC BER threshold, there is a maximum value of $OSNR_{\text{TOT}}$ penalty that can be tolerated: for values higher than this maximum, the system becomes unfeasible.

D. Comments

The most relevant features of the two analyzed network planning strategies are summarized in Table II.

In case of minimum BER, the optimization is local and the optimum launched power in each span depends only on the characteristics of the span, also in cases of multi-span systems with different η in each span. The value of $OSNR_{\text{NL,opt}}$ changes with the number of spans: it is not an invariant for the link optimization (the optimum power is the invariant) and each span contributes to the $OSNR_{\text{NL,opt}}$ depending on its value of η and $P_{\text{Tx,opt}}$.

In case of maximum OSNR margin, the invariant for the optimization is $OSNR_{\text{NL}}$, regardless of the number of spans and their coefficient η : it depends only on TXP linear performance at FEC BER threshold.

In a multi-span system with different values of η in each span, the optimum launched power in each span has to satisfy the relationship:

$$\sum_{k=1}^{N_{\text{span}}} (P_{\text{Tx}}^{(k)})^2 \eta^{(k)} = OSNR_{\text{NL,opt}}^{-1} \quad (14)$$

TABLE II
CHARACTERISTICS OF PLANNING STRATEGIES

	Maximum OSNR margin	Minimum BER
Optimization strategy	Global @ link level	Local @ span level
Optimum working point	For each <u>optical circuit</u> : $OSNR_{\text{NL,opt}} = 3 \cdot OSNR_{\text{FEC}}$	For each span: $P_{\text{opt}}^m = \sqrt[3]{h \nu F A_{\text{span}} / 2 \cdot \eta}$
Non-linear OSNR penalty	1.8dB @ $OSNR_{\text{FEC,NL}}$	1.8 dB @ $OSNR_{\text{ASE,Rx}}$
Margins sensitivity around optimum power	$P_{\Delta} = \Delta \cdot P_{\text{opt}}^M$ Delta $OSNR_{\text{margin}}$: $\frac{\Delta(3 - \Delta^2)}{2}$	$P_{\Delta} = \Delta \cdot P_{\text{opt}}^m$ Delta $OSNR_{\text{tot}}$: $\frac{3\Delta}{(2 + \Delta^3)}$

As a consequence, the optimum power in each span depends on a global optimization law. In case of homogeneous systems, it is instead possible to derive the optimum value of launched power using Eq. (8).

IV. DYNAMIC NETWORK PLANNING

Recent developments of optical technologies enabled dynamic optical networking, in which optical networks can evolve in time accommodating new traffic requests. Thanks to the presence of elastic transponders [9], the user can modify the bit rate of optical signals by selecting a proper modulation formats and/or modify the traffic matrix connecting source nodes to destination nodes over optical paths which were not envisaged during the first deployment phase. Also, it will be possible, after restoration events, to reroute the existing traffic over alternative available paths, not validated during the network design phase. Moreover, the availability of flex-spectrum technologies, combined with the full tunability of transponders, enables a full dynamic adaptation of the network also in terms of spectral occupancy in order to maximize the spectral efficiency.

This increased flexibility could be exploited to reduce the overall network costs: in fact, it allows simultaneously maximizing the transmission performances and minimizing the number of regenerators needed to support the requested traffic matrix.

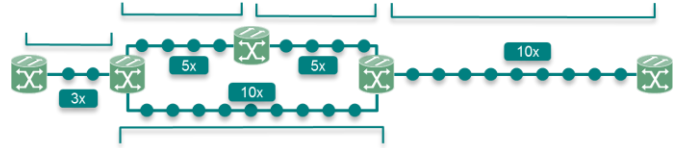


Fig. 5. Traffic distribution in the reference scenario (Nx indicates a network segment composed of N spans).

The goal of analysis reported in this section is to identify the best network planning strategy which maximizes the degree of dynamic adaptation of the network. In particular, we will compare the two planning strategies introduced in

Section III in a reference network where:

- An initial traffic matrix is defined, together with the minimum spacing and the maximum number of channels to be guaranteed in each add/drop section over the entire operative life of the system.
- The transmission fiber type is fixed.
- The amplification layer is characterized in terms of the noise figure (F) of the deployed amplifiers (for simplicity, but without loss of generality, we assume the use of ideal amplifiers whose F is independent of the gain).

For the network with the traffic matrix defined in a first provisioning phase, the amplifier settings (i.e. the values of the fiber launched power P_{Tx}) are evaluated in order either to maximize the OSNR margin or to minimize the BER, taking into account the accommodation of the full traffic load requested by the user (power optimization for full channel load planning).

Three different evolution scenarios are studied:

- Evolution of traffic matrix: new optical path, different modulation formats and new sources of linear penalty – see Section IV.B.
- Amplifier layer behavior: accommodation of amplifier tilt and ripple, accuracy in power settings and transient management – see Section IV.C.
- Span losses variation – see Section IV.D.

In each case, system robustness in case of maximum OSNR margin planning is compared with system robustness in case of minimum BER planning.

A. The Reference Scenario

The reference network is shown in Fig. 5, where the wavelength cross-connect (WXC) sites are indicated with the cross-connection symbols, whilst the amplification sites are indicated with full circles and each of them hosts an EDFA amplifier with $F=5$ dB. The transmission spans (assumed identical for simplicity) are composed of uncompensated single-mode fiber (SMF) spans with length 80km and a span budget $A_{span}=15$ dB. The full-load traffic matrix is composed of 80 channels in a 50-GHz grid. The first provisioning traffic uses 100Gb/s CP-DQPSK TXP's with a linear performance at the FEC correction threshold ($BER=4e-3$) equal to $OSNR=8$ dB over 0.5nm.

Fig. 6 reports the estimated performance for 3x, 5x and 10x links in a full-load configuration with a network planning strategy at maximum OSNR margin (in green) and minimum BER (in blue). In case of maximum OSNR margin planning, different optical paths have the same optimum non-linear power P_{NLI} (i.e. they lay on the same BER vs. $OSNR_{ASE}$ curve) and the same non-linear penalty, measured at the FEC threshold. The OSNR margin scales as a function of the $OSNR_{ASE,Rx}$, i.e. of the number of spans. This behavior is strictly related to the fact that signals with the same linear performance (same $OSNR_{FEC}$) are transmitted over the different links. Moreover, the optimum launched power is different in each link, depending on the number of spans: since the total P_{NLI} is constant and since the value of P_{NLI} generated in each span is the same (the system is composed of identical spans), if the number of spans increases, the contribution of each span to P_{NLI} has to

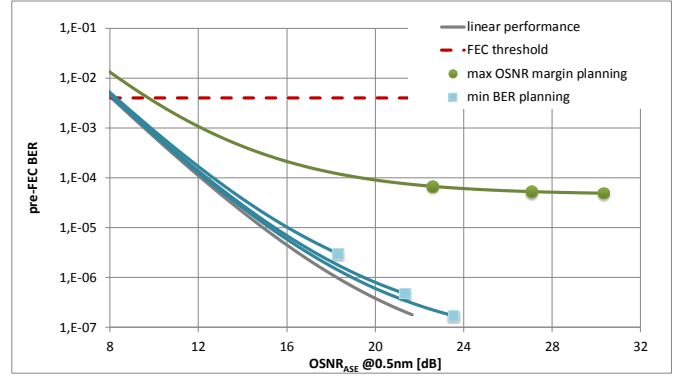


Fig. 6. BER vs. $OSNR_{ASE}$ in the reference scenario of Fig. 5 when the two planning strategies are used (blue lines: pre-FEC BER vs. $OSNR_{ASE}$ curves at minimum BER planning, green line: pre-FEC BER vs. $OSNR_{ASE}$ curves at maximum OSNR margin planning; markers: working points for each considered optical path).

decrease, thus the optimum launched power decreases, as well (see Eq. (3)).

On the contrary, in case of minimum BER planning, the optimum launched power remains constant, regardless of the number of spans (see Eq. (9)), inducing a change, in each link, of the optimum value of P_{NLI} . This implies that the different optical paths are characterized by different BER vs. $OSNR_{ASE}$ curves. However, the non-linear penalty at the optimum working point is kept constant and equal to approximately 1.8dB, as shown in Section III.B.

Starting from this network configuration, several scenarios of dynamic evolution will be considered. In each case, the transmission performance in the new configuration will be evaluated, either using the maximum OSNR margin or the minimum BER planning strategy, assuming to keep the optimum power fixed at the value evaluated in the first network planning. In particular:

- Per channel powers are assumed to be the optimum powers at maximum OSNR margin or at minimum BER imposed by present traffic planning.
- “New traffic is provisioned” / “physical layer modifications are evaluated” in the hypothesis the target per channel powers are unchanged.
- Margin's variations of the traffic in the new configuration are compared in case of planning at maximum OSNR margin or minimum BER to identify criticalities of the two different approaches when installed networks dynamically evolve.

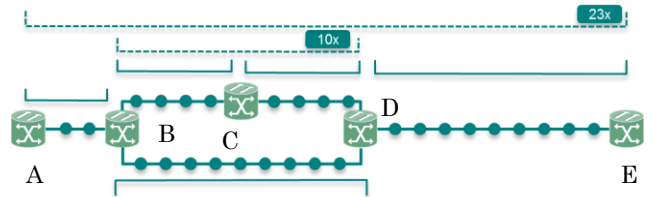


Fig. 7. New traffic distribution (Nx indicates a network segment composed of N spans).

B. Evolution of traffic matrix

In order to cope with requests of traffic variations, over the operative life of a network the traffic matrix can vary in order to accommodate new requirements. Starting from the reference scenario described in Section V.A, in a first example we assume that a part of the traffic deployed in the first provisioning phase (solid line link in Fig. 7) is replaced by the new dashed optical paths. The transmission performances of the new optical paths, evaluated in a full-load condition, are reported in Fig. 8, where “full-load” means that in each section of the network a total of 80 channels are present, which in general may follow different paths.

In case of maximum OSNR margin planning (green lines in Fig. 8), the OSNR margin of future traffic rapidly decrease and the longest link is unfeasible; this is because planning for the maximum OSNR margin optimizes specific traffic configuration: any other links having different path on the same network is in sub-optimum conditions with respect to OSNR margin.

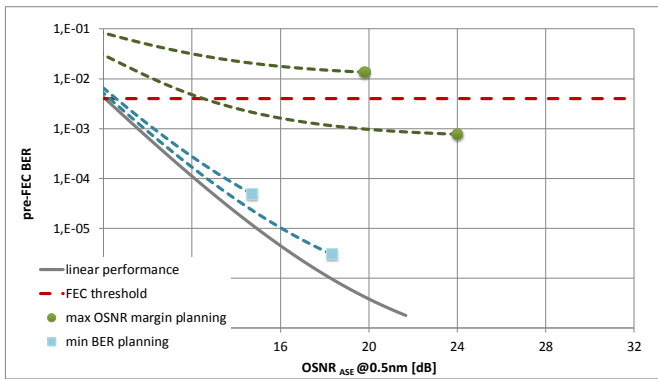


Fig. 8 Transmission performance of the new optical paths shown as dashed lines in Fig. 7, evaluated in a full-load condition (blue lines: pre-FEC BER vs. OSNR_{ASE} curves at minimum BER planning, green line: pre-FEC BER vs. OSNR_{ASE} curves at maximum OSNR margin planning; markers: working points for each considered optical path).

In case of minimum BER planning (blue lines in Fig. 8), new demands are always working at the maximum Q margin; the longest link is feasible. This because planning at minimum BER selects optimum powers only depending on amplification layer (that remains unchanged).

In a second example, we assume that, thanks to the use of reconfigurable cards, the traffic capacity transmitted over the D to E link in Fig. 7 can be increased, going from the 100Gb/s CP-DQPSK to 200Gb/s CP-16QAM modulation format. In Fig. 9, the transmission performance of the full-load system employing the new modulation format, under the hypothesis of first planning at maximum OSNR margin (solid line) and minimum BER (dash-dotted line), assuming a minimum required OSNR at the FEC threshold equal to 8.2dB (at 100Gb/s) or 13dB (at 200Gb/s) over a 0.5nm bandwidth. The performance is compared to the one achieved by 100Gb/s CP-DQPSK over the same link and under the same conditions.

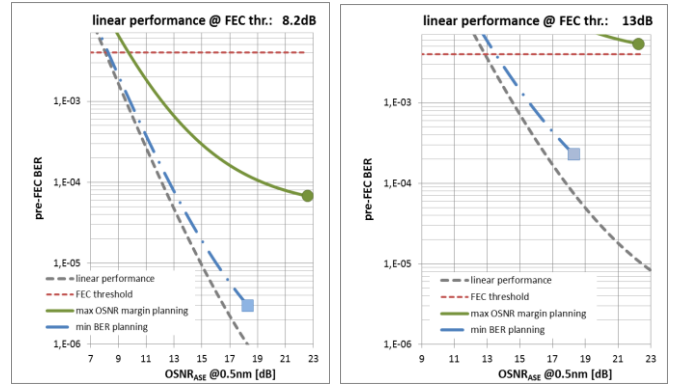


Fig. 9 Transmission performance vs. OSNR_{ASE} of the full-load system employing the new modulation format, under the hypothesis of first planning at maximum OSNR margin (solid line) and minimum BER (dash-dotted line). Dashed lines: TXP’s linear performance. Markers: working points for each considered optical path.

In case of maximum OSNR margin planning, the OSNR margin of new modulation formats decreases and the link requiring a higher OSNR in linear condition is unfeasible. This happens because planning at maximum OSNR margin depends on TXP linear performance, OSNR_{FEC}. In case of minimum BER planning, new demands are always working at the minimum BER; this because planning at minimum BER selects optimum powers independently of card linear performance. The same behavior is obtained in case of degradations of the linear performance of the system, due for instance to additional sources of linear crosstalk, which similarly result in an increase of the value of OSNR_{FEC}.

In conclusion, minimum BER network planning allows the modified traffic matrix service to always work at minimum BER condition, since the optimum power is independent of both number of spans and TXP performance. On the contrary, networks planned in first provisioning using the maximum OSNR margin strategy, turns out to have a low degree of flexibility whenever, along the operative life of the system, a variation of the traffic matrix is required: since the optimum power, which maximizes the OSNR margin, is strictly dependent on the value of OSNR_{FEC} and N_{span} , the performance becomes suboptimum whenever the optical path or the TXP type is modified, potentially making unfeasible links that would have been functioning if the minimum BER planning strategy was used. In order to recover the optimum working point in the maximum OSNR margin condition, a re-optimization of the network would be required with a new provisioning of fiber launch power that could modify the operational settings of the amplifiers for all channels in partial or total overlap with the new required traffic (i.e. a global optimization of the network in order to keep the total P_{NLI} of each optical path to the optimum value). This re-optimization can be critical because it modifies the amplifier’s operative setting of live traffic.

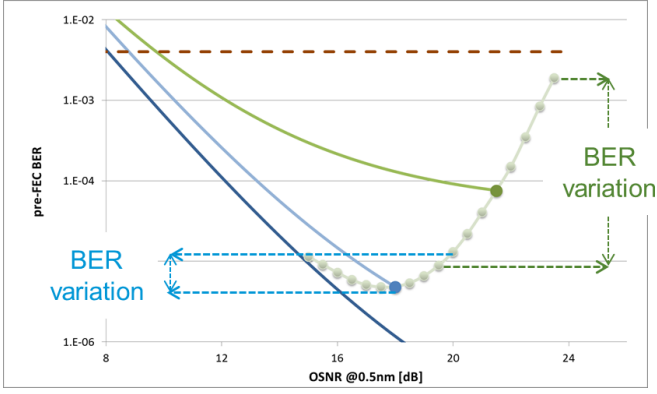


Fig. 10 BER performance variations vs. accuracy of amplifier power settings. In x-axis the $OSNR_{ASE}$. Blue: minimum BER planning; Green: maximum OSNR margin planning; Grey: performance at different power in fiber with incremental step of 0.5dB (see the text for more details).

C. Amplifier layer behavior

Accuracy in the amplifier settings and amplifier's control during fast variation of the number of amplified channels are the main sources of deviations of per channel powers with respect to the target. In this section we investigate the performances degradation of transmitted signals comparing maximum OSNR and minimum BER planning strategies using, as example, the 10x link of Fig. 6 (link D-E).

Per channel power deviations at the amplifier output with respect to required target values are mainly due to:

- accuracy of per channel power settings;
- amplifier tilt and inter-channel Raman tilt;
- amplifier ripple.

Depending on the channel position (in frequency) in the DWDM spectrum, the current channel power can be greater or lower than the target per channel power. Also, due to tilt and ripple effects, the offset with respect to the target of the current channel power is common to a significant subset of adjacent channels (in a few hundreds GHz around the channel under test).

To evaluate the system robustness to power offset with respect to the target, the margins variations around the optimum are compared assuming, for simplicity, that all the channels of the DWDM spectrum suffer the same power offset. For sake of simplicity, the same power offset of ± 2 dB have been applied in all the spans of the link; this is a worst case approximation of what happens in a real system where the power offset increases span per span along the link. Nevertheless, to compare in principle the robustness to power setting accuracy of the two different planning strategies, this simplified analysis could be useful. The results are shown in Fig. 10: blue and green dots quote the performance of the link when the amplifiers settings perfectly match the target optimum ones; dots in gray quote the performance variations as a consequence of changes of the per channel power (each point differs from the adjacent of 0.5dB of in fiber per channel power). BER variations have been compared assuming the same power uncertainty range both at maximum OSNR margin and minimum BER planning.

These results can be analyzed based on Eq. (12) and Eq. (13):

- At minimum BER planning, $OSNR_{TOT}$ reduction is independent of the received OSNR (i.e., span loss and F), as shown in Eq. (13) and in Fig. 4. In terms of $OSNR_{TOT}$ reduction, ± 2 dB of power setting accuracy reflects into a degradation of 0.75/1 dB.
- At maximum OSNR margin planning, the OSNR margin reduction is independent of the received OSNR; nevertheless, changing the received OSNR, the same OSNR margin reduction implies different Q margin reduction. Furthermore, when the launched power locally exceeds by 2.38dB the optimum power, the floor condition is reached (see Eq. (12) and Fig. 3). Note that typical peak-to-peak ripple values for a cascade of 10 amplifiers are of the order of ± 2 dB.

In conclusion, minimum BER planning is more robust to power variations around the optimum than maximum OSNR margin planning.

As a second example, we assess the effects of the dynamic transient control of the amplifiers after fast reduction of input power (e.g. the fast reduction of amplifier input power can occur during fiber cuts that suddenly drop a significant part of channels in the DWDM spectrum). As a worst case scenario, we assume that the network is working with the DWDM spectrum fully populated of channels (full load condition); in the example, the reference link is the D-E 10x in Fig. 6 with 80 channels at 50GHz-spacing and using the same modulation format. We assume, as case study, a fiber cut occurring in the multiplexing DWDM section where a subset of channels is instantaneously dropped and the surviving channels remain at 50GHz spacing; the surviving channels suffer power undershoot and overshoot due to amplifier transient control. During this transient, surviving channels suffer $OSNR_{ASE}$ variation due to power variation and, simultaneously, $OSNR_{NL}$ variation due to both in fiber power variation and non-linearity coefficient variation (this last variation is due to the fact that a reduced number of interfering channels reduces non-linear multi-channel effects).

Scope of the analysis is the performances comparison of the surviving channels during transient in two cases: the link at full load is operating at the optimum power for OSNR margin optimization and the link at full load is operating at the optimum power for BER minimization. To model the transient behavior we assume that:

- During the transient, each amplifier of the line scales the per-channel output power of a factor δ so that, for the amplifier at the input of the k-th span, $P^{(k)} = \delta^k P_{target}^{(k)}$.
- The factor δ scales with the number of dropped channels, N_d ; we assumed a linear dependence between δ and the number of dropped channels, with $\delta=1$ at $N_d=0$.
- The non-linearity coefficient $\eta_{full\ load}$ is reduced of a factor χ to take into account the non-linear effects mitigation due to the reduction of number of channels, $\eta_{current\ load} = \chi \cdot \eta_{full\ load}$. χ values have been computed assuming the surviving channels are all adjacent in the 50GHz grid (worst case condition);

these values refer to the central channel of the surviving DWDM part of the spectrum.

Under these hypotheses we can demonstrate (see Appendix E) that, during transient, at maximum OSNR margin planning, the total OSNR margin reduction with respect to the OSNR margin at full load is equal to:

$$\frac{OSNR_{margin}^{transient}}{OSNR_{margin}^{full\ load}} = \frac{3}{2} \frac{1 - \frac{1}{\delta}}{\frac{1}{\delta} - \left(\frac{1}{\delta}\right)^{N_{span}+1}} \left(N_s - \frac{\chi}{3} \frac{\delta^2 - \delta^{2(N_{span}+1)}}{1 - \delta^2} \right) \quad (15)$$

while, at minimum BER planning, the total OSNR reduction with respect to the total OSNR at full load is equal to:

$$\frac{OSNR_{tot}^{transient}}{OSNR_{tot}^{full\ load}} = \frac{3}{2} N_s \left(\frac{\frac{1}{\delta} - \left(\frac{1}{\delta}\right)^{N_{span}+1}}{1 - \frac{1}{\delta}} + \frac{\chi}{2} \cdot \frac{\delta^2 - (\delta^2)^{N_{span}+1}}{1 - \delta^2} \right) \quad (16)$$

In Fig. 11, the performance variation of surviving channels is evaluated for different values of δ , in order to emulate different magnitudes of power undershoot and overshoot at the end of the link of 10 amplifiers; we selected a δ range of [0.9 - 1.15], corresponding to delta power at the output of the last amplifier of [-4.6 - 6] dB when only one channel survives.

Results are compared in case of planning at maximum OSNR margin (Fig. 11 a) and minimum BER (Fig. 11 b). Results show that planning at minimum BER is more robust to transient effects; a maximum margin reduction of 1 dB is required to compensate performances degrade. On the opposite, at maximum OSNR margin planning, power overshoots are rapidly impacting performances when the overshoots are in the upper limit value of the considered region. Finally, we notice that also undershoots can significantly impact performances, due to $OSNR_{ASE, Rx}$ reduction.

D. Span losses variations

During the system operative life-time, the optical links evolves progressively increasing the loss of each span, e.g. due to aging and fiber cuts.

The traffic demand performances degradation due to aging is studied considering the evolution from a BOL (beginning of life) scenario planned at maximum OSNR margin and at minimum BER to an EOL (end-of-life) scenario. The reference link is the 10x (D to E in Fig. 5) with an increase of A_{span} from 15 dB at BOL to 20 dB at EOL (end of life) in all spans.

Results are shown in Fig. 12. At maximum OSNR planning, the OSNR margin maximization condition is achieved when the link cumulates the total non-linear noise of Eq. (7); as $OSNR_{NL,opt}$ is independent from A_{span} , even changing the span loss, the link is always working at the optimum condition: margin is always at the maximum and the optimum power remains unchanged; the amplifiers settings are unchanged, as well, without modifications in the system configuration.

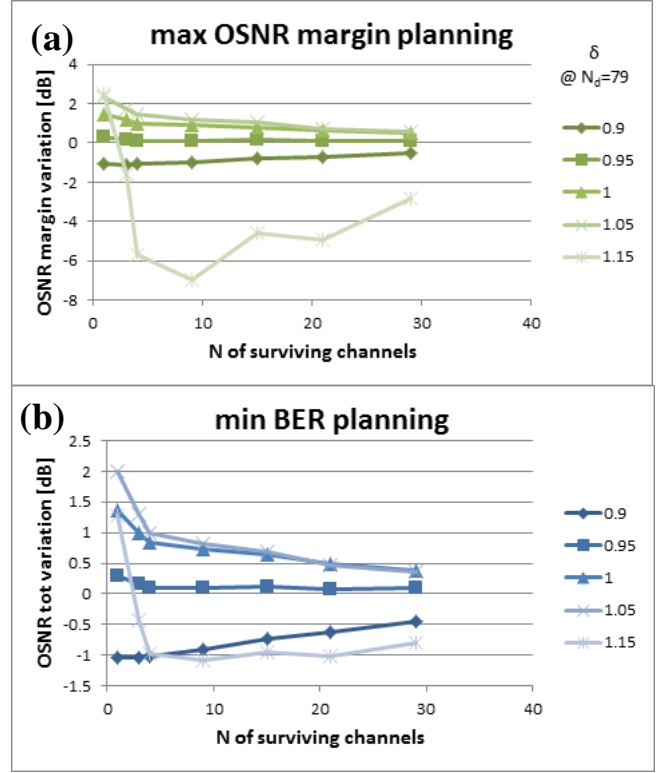


Fig. 11 (a) Variation of $OSNR_{margin}$ as a function of the number of surviving channels in case of planning at maximum OSNR margin. (b) Variation of $OSNR_{tot}$ as a function of the number of surviving channels in case of planning at minimum BER. Each curve corresponds to a different value of δ when $N_d=79$ (see text for details).

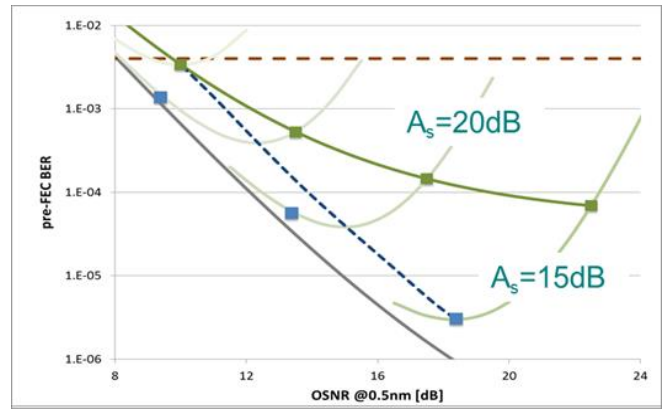


Fig. 12 Effects of span losses variation in case of planning at minimum BER (blue dots) and maximum OSNR margin (green dots). Thin grey curves: system working points at different span losses. Dashed blue curve: performance at minimum BER planning if the power is continuously adapted to compensate span loss variations.

In case of minimum BER planning, to achieve the optimum performance, power has to be changed when span loss changes. If power is kept constant at the BOL optimum condition, increasing the span loss the performance degrades with respect to the performance we can achieve

with the new optimum power. The $OSNR_{tot}$ reduction with respect to the optimum power at each span loss slowly increases: a variation of A_{span} equal to ± 3 dB requires a variation in power equal to ± 1 dB, that corresponds to a variation in $OSNR_{tot}$ of ± 0.25 dB; nevertheless, this minimal sub-optimization, can significantly impact the overall performance if we add the impact of power setting uncertainties, e.g., for tilt and ripple accommodation). As shown in Fig. 12, progressively increasing the span loss and suitably modifying the optimum power in case of minimum BER planning (dashed blue curve), the working point at minimum BER converges on the working point at maximum OSNR margin. In this case, at FEC BER threshold, the penalty in $OSNR_{NL}$ is equal to 1.8dB, and coincides with system penalty at $OSNR_{ASE,Rx}$.

E. Comments

Table III reports a comparison between the maximum OSNR margin and minimum BER strategies, summarizing the main pros and cons of the two methods.

TABLE III
PROS AND CONS OF PLANNING STRATEGIES

	Maximum OSNR margin	Minimum BER
P R O S	Optimum solution to accommodate span losses variation w/o changes in the settings of the amplification layer.	Best optical performance and robustness to power fluctuations, whatever is the new provisioned traffic, without changes in the settings of the amplification layer.
C O N S	Adaptive change of amplifiers working points required during the provisioning of new traffic. Low robustness to power fluctuations.	In case of losses variation, changes in the settings of the amplification layer required to guarantee the optimum performance

In case of dynamical network management, maximum OSNR margin planning requires adaptive change of amplifiers working point every time we ask the provisioning of new traffic with different path and different OSNR at FEC correction limit, with respect to present traffic. In case we cannot change the amplifiers settings, new provisioned traffic underperforms and/or new channels cannot be validated. Furthermore, the accommodation of power deviation from the optimum target can be critical. For a fixed traffic matrix, maximum OSNR planning is the best solution to accommodate span losses variation from BOL to EOL condition.

On the contrary, in case of dynamical network management, minimum BER planning assures the achievement of best performance, whatever is the new provisioned traffic, and the best system robustness to power fluctuations, without changes in the setting of the amplification layer.

In case of loss variations from BOL to EOL condition,

minimum BER planning underperforms if powers are not modified to adapt amplifier settings at the current network configuration. This means that to always assure the best traffic performance, when span losses change the amplifiers settings have to be changed. As span loss variation typically occurs after fiber cut, significant changes in power settings occur after disrupting traffic events (no major impact on system with live traffic).

The minimum BER planning is the best solution for dynamic network management; the availability of a power control layer tracking current span losses allows the power dynamical adjustment and guarantee the system is working at the optimum performance. Its main drawback is the dependence on the optimum P_{Tx} on the span loss (see Eq. (8)). However, it has been shown in [10] that an automatic gain control, *locally* tracking the span loss variation and adjusting the power at the output of the amplifier, is sufficient to recover the working point at minimum BER. On the contrary, a re-optimization of the network using the maximum OSNR margin planning would require, for a single span loss variation, power changes in every span of the network.

V. NETWORK PLANNING FOR MAXIMUM REACH

If we assume to operate at the FEC correction threshold, i.e. with both OSNR and BER margin equal to zero, the minimum BER and maximum OSNR margin approaches converge to the same value of optimum launched power (i.e. in the value of power obtained with Eq. (9) is equal to the one obtained with Eq. (8)). This condition corresponds to the system maximum reach, i.e., the maximum length of the link that can be achieved, increasing the number of spans at fixed insertion loss or increasing the span loss to use system margins in case the number of span is fixed. The maximum reach scales with the linear performance of the card at FEC correction limit and with amplification layer characteristics, according to the following relationship (that can be derived imposing that P_{opt}^M given in Eq.(8) is equal to P_{opt}^m given in Eq.(9)):

$$N_{span} \cdot (A_{span})^{2/3} = \frac{2}{3} \cdot \frac{1}{OSNR_{FEC}} \cdot \frac{1}{B_n \cdot (h\nu \cdot F)^{2/3}} \cdot \frac{1}{(2\eta)^{1/3}} \quad (17)$$

For a fixed span loss, the number of spans increases either when the OSNR at FEC correction threshold decreases (1 dB of $OSNR_{FEC}$ improvement reflects into 1 dB of N_{span} improvement) or when the amplifier NF decreases (3dB of F improvement reflects into 2dB of N_{span} improvement). For a fixed number of spans, the span loss increases either when the OSNR at FEC correction threshold decreases (2 dB of OSNR improvement reflects into 3 dB of A_{span} improvement) or when the amplifier F decreases (1 dB of F improvement reflects into 1dB of improvement in A_{span}).

An experimental validation of the accuracy of Eq. (17) in the prediction of maximum reach vs. span-loss performance has been reported in [3]. The good agreement between the experimental results shown in [11] and the predictions of Eq. (17) confirmed the reliability of the analytical formula.

A. Estimation of network costs

Eq. (17) is also a simple but accurate tool for the estimation of the network costs, since it contains all relevant system parameters and their relationship to traffic performance. An example of this application is summarized in Fig. 13 where the formula has been applied to evaluate the network costs (in terms of number of TXPs and number of amplification sites) in a submarine transmission system composed of 6000 km of pure-silica-core fiber. The number of repeaters (i.e., amplification sites) has been computed changing the number of channels in the DWDM spectrum to fit the full capacity request of 5 Tb/s: this can be achieved by means of Nyquist elastic cards working at 32 Gbaud that modulate the channel bit-rate in the range 50 Gb/s to 200 Gb/s. Channels are assumed equally spaced in the EDFA amplifier's bandwidth of 3.7 THz and NF is set to 4 dB. Increasing the channel bit rate, the number of TXPs and the non-linear coefficient η accordingly decreases; nevertheless, increasing the channel bit rate, due to higher OSNR_{FEC} , the number of spans satisfying Eq. (17) increases, as shown in Fig. 13.

In each of the four possible solutions, the overall network cost can be derived: the different scenarios can be compared in terms of investment for amplification layer infrastructure and TXPs to support first traffic installation. Furthermore, the TXPs costs evolution based on forecast traffic requests can be studied.

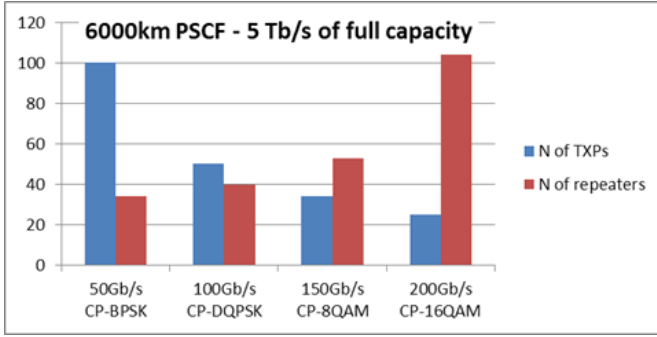


Fig.13 . Submarine transmission system of 6000km of pure-silica fiber ($\alpha=0.17$ dB/km, $D=20.9$ ps/mn/km, $A_{\text{eff}}=130$ μm^2). $\text{OSNR}_{\text{FEC}} = [2.5, 6.5, 10, 14]$ dB @0.5nm for [50, 100, 150, 200]Gb/s respectively.

VI. CONCLUSION

In pure coherent uncompensated optical networks it is necessary to identify planning strategies able to maximize performances at network planning and manage the dynamic evolutions of the network during its operative life.

We proposed two alternative approaches: the first one maximizing the OSNR margins, the second one minimizing received BERs. In both cases, analytical formulas have been derived. Furthermore, a closed-form expression for the maximum reach (in terms of number of spans and loss budget) of each interface has been given; this closed formula has been used to evaluate overall network cost in a reference scenario.

The two proposed strategies have been compared

studying the sensitivity to dynamic evolution of a reference network with respect to traffic matrix changes, amplification layer stability and span loss variations. The adaptive minimum BER planning has been shown to be the best planning strategy for dynamic meshed flexible networks.

APPENDIX

A. Maximization of OSNR margin

For a generic multi-span system, the maximization of the OSNR margin is equivalent to the maximization of:

$$\text{OSNR}_{\text{margin}} = \frac{\text{OSNR}_{\text{ASE,Rx}}}{\text{OSNR}_{\text{FEC,NL}}} \quad (18)$$

where:

$$\begin{aligned} \frac{1}{\text{OSNR}_{\text{FEC,NL}}} &= \frac{1}{\text{OSNR}_{\text{FEC}}} - \sum_{k=1}^{N_{\text{span}}} \frac{1}{\text{OSNR}_{\text{NL}}^{(k)}} = \\ &= \frac{1}{\text{OSNR}_{\text{FEC}}} - \sum_{k=1}^{N_{\text{span}}} \eta^{(k)} B_n (P_{\text{Tx}}^{(k)})^2 \end{aligned} \quad (19)$$

$$\frac{1}{\text{OSNR}_{\text{ASE,Rx}}} = \sum_{k=1}^{N_{\text{span}}} \frac{1}{\text{OSNR}_{\text{ASE,Rx}}^{(k)}} = \sum_{k=1}^{N_{\text{span}}} \frac{P_{\text{ASE}}^{(k)}}{P_{\text{Tx}}^{(k)}} \quad (20)$$

$$P_{\text{Tx}}^{(k)} = \left(\frac{1}{\eta^{(k)} B_n} \right)^{1/2} \left(\frac{1}{\text{OSNR}_{\text{NL}}^{(k)}} \right)^{1/2} \quad (21)$$

The maximization of the OSNR margin defined in Eq. (18) corresponds to the identification of the value of OSNR_{NL} (or, equivalently, $1/\text{OSNR}_{\text{NL}}$) which maximizes the $\text{OSNR}_{\text{margin}}$:

$$\text{OSNR}_{\text{margin}} = \frac{\sum_{k=1}^{N_{\text{span}}} P_{\text{ASE}}^{(k)} (\eta^{(k)} B_n)^{1/2} \left(\frac{1}{\text{OSNR}_{\text{NL}}} \right)^{-1/2}}{\left(\frac{1}{\text{OSNR}_{\text{FEC}}} - \sum_{k=1}^{N_{\text{span}}} \frac{1}{\text{OSNR}_{\text{NL}}^{(k)}} \right)} \quad (22)$$

Forcing the derivative of Eq.(22) with respect to $1/\text{OSNR}_{\text{NL}}^{(j)}$ to be equal to zero, we get, at the optimum:

$$\begin{aligned} \frac{1}{2} P_{\text{ASE}}^{(j)} \cdot (\eta^{(j)} B_n)^{1/2} \left(\frac{1}{\text{OSNR}_{\text{NL,opt}}^{(j)}} \right)^{-3/2} \left(\frac{1}{\text{OSNR}_{\text{FEC}}} - \sum_{k=1}^{N_{\text{span}}} \frac{1}{\text{OSNR}_{\text{NL,opt}}^{(k)}} \right) &= \\ = \sum_{k=1}^{N_{\text{span}}} P_{\text{ASE,opt}}^{(k)} \cdot (\eta^{(k)} B_n)^{1/2} \left(\frac{1}{\text{OSNR}_{\text{NL,opt}}^{(k)}} \right)^{-1/2} &\quad \forall j = 1, \dots, N_{\text{span}} \end{aligned} \quad (23)$$

Using Eqs. (19) and (20), the previous expression can be rewritten as:

$$\left(\frac{1}{\text{OSNR}_{\text{NL,opt}}^{(j)}} \right)^{-3/2} = 2 \cdot \frac{\text{OSNR}_{\text{FEC,NL}}}{\text{OSNR}_{\text{ASE,Rx}}} \frac{1}{P_{\text{ASE,opt}}^{(j)} \cdot (\eta^{(j)} B_n)^{1/2}} \quad (24)$$

For $j=1, \dots, N_{\text{span}}$. Combining Eq. (21) and Eq. (24), we get:

$$P_{\text{opt}}^{(j)} = \sqrt[3]{\frac{\text{OSNR}_{\text{ASE,Rx}}}{2 \text{OSNR}_{\text{FEC,NL}}} \cdot \frac{P_{\text{ASE,opt}}^{(j)}}{\eta^{(j)} B_n}} \quad \forall j = 1, \dots, N_{\text{span}} \quad (25)$$

At the optimum condition, the optimum non-linear OSNR is equal to:

$$\frac{1}{\text{OSNR}_{\text{NL,opt}}} = \sum_{j=1}^{N_{\text{span}}} \eta^{(j)} B_n (P_{\text{Tx,opt}}^{(j)})^2 \quad (26)$$

Substituting Eq. (25) in Eq. (26), we get:

$$\begin{aligned} \frac{1}{\text{OSNR}_{NL}^{opt}} &= \sum_{j=1}^{N_s} \frac{\eta^{(j)} B_n (P_{Tx, opt}^{(j)})^3}{P_{Tx, opt}^{(j)}} = \\ &= \frac{1}{2} \frac{\text{OSNR}_{ASE, Rx}}{\text{OSNR}_{FEC, NLopt}} \sum_{j=1}^{N_s} \frac{P_{ASE, opt}^{(j)}}{P_{Tx, opt}^{(j)}} = \frac{1}{2} \frac{1}{\text{OSNR}_{FEC, NLopt}} \end{aligned} \quad (27)$$

Since

$$\frac{1}{\text{OSNR}_{FEC, NLopt}} = \frac{1}{\text{OSNR}_{FEC}} - \frac{1}{\text{OSNR}_{NL}^{opt}} \quad (28)$$

from Eq. (27) we get:

$$\frac{1}{\text{OSNR}_{NL, opt}} = \frac{1}{2} \left(\frac{1}{\text{OSNR}_{FEC}} - \frac{1}{\text{OSNR}_{NL}^{opt}} \right) \quad (29)$$

or, equivalently,

$$\text{OSNR}_{NL}^{opt} = 3 \cdot \text{OSNR}_{FEC} \quad (30)$$

In case if identical spans, since

$$\text{OSNR}_{NL} = \frac{P_{Tx}}{P_{NL}} = \frac{1}{B_n \eta \cdot N_{span} P_{Tx}^2} \quad (31)$$

It is finally easy to derive the optimum value of launched power corresponding to the optimum value of non-linear OSNR of Eq. (31) as:

$$P_{opt}^M = \sqrt[3]{\frac{1}{3 \cdot \text{OSNR}_{FEC}} \frac{1}{B_n \eta \cdot N_{span}}} \quad (32)$$

B. Minimization of BER

The minimization of the pre-FEC BER is equivalent to the maximization of the total OSNR, where (for a generic multi-span system):

$$\frac{1}{\text{OSNR}_{tot}} = \sum_{k=1}^{N_{span}} \frac{1}{\text{OSNR}_{ASE, Rx}^{(k)}} + \sum_{k=1}^{N_{span}} \frac{1}{\text{OSNR}_{NL}^{(k)}} \quad (33)$$

with:

$$\text{OSNR}_{ASE, Rx}^{(k)} = \frac{P_{Tx}^{(k)}}{h\nu B_n G^{(k)} F^{(k)}} \quad (34)$$

$$\text{OSNR}_{NL}^{(k)} = \frac{1}{B_n \cdot \eta^{(k)} \cdot (P_{Tx}^{(k)})^2}$$

The maximization of OSNR_{tot} corresponds to finding the optimum value of launched power in each span which minimizes the right part of Eq. (33). This can be obtained by maximizing, for each span, the local OSNR (as also shown in [8]), i.e. by minimizing:

$$\frac{1}{\text{OSNR}_{tot}^{(k)}} = \frac{1}{\text{OSNR}_{ASE, Rx}^{(k)}} + \frac{1}{\text{OSNR}_{NL}^{(k)}} \quad (35)$$

Substituting Eq. (34) in Eq. (35) and forcing the derivative with respect to P_{Tx} to be equal to zero, we get:

$$\left(-\frac{h\nu B_n A_{span}^{(k)} F^{(k)}}{(P^{(k)})^2} + 2 \cdot B_n \eta^{(k)} \cdot P_{Tx}^{(k)} \right) = 0 \quad \forall k = 1, \dots, N_{span} \quad (36)$$

The solution of Eq. (28) yields the optimum value of launched power in each span:

$$P_{opt}^{(k)} = \left(\frac{h\nu A_{span}^{(k)} F^{(k)}}{2\eta^{(k)}} \right)^{1/3} \quad (37)$$

It's easy to verify that, at the optimum transmission power, the amount of ASE noise is always twice the amount of non-linear noise [12] or, equivalently:

$$\text{OSNR}_{NL}^{(k)} = 2 \cdot \text{OSNR}_{ASE, Rx}^{(k)} \quad (38)$$

C. OSNR non-linear penalty

When the maximum OSNR margin strategy described in Section III.A is used, the OSNR non-linear penalty at the FEC correction threshold is defined as:

$$\text{OSNR}_{pen} = \frac{\text{OSNR}_{FEC, NL}}{\text{OSNR}_{FEC}} \quad (39)$$

with:

$$\frac{1}{\text{OSNR}_{FEC, NL}} = \frac{1}{\text{OSNR}_{FEC}} - \frac{1}{\text{OSNR}_{NL}^{opt}} \quad (40)$$

Using the result of Eq. (30), we obtain:

$$\text{OSNR}_{pen} = 2/3 \approx 1.8\text{dB} \quad (41)$$

When the minimum BER strategy described in Section III.B is used, the OSNR non-linear penalty at the minimum BER working point is defined as:

$$\text{OSNR}_{pen} = \frac{\text{OSNR}_{ASE, Rx}}{\text{OSNR}_{tot, RX}} \quad (42)$$

with:

$$\frac{1}{\text{OSNR}_{tot, RX}} = \frac{1}{\text{OSNR}_{ASE, Rx}} + \frac{1}{\text{OSNR}_{NL}^{opt}} \quad (43)$$

Using the result of Eq. (38), we again obtain:

$$\text{OSNR}_{pen} = 2/3 \approx 1.8\text{dB} \quad (44)$$

D. Sensitivity to power variation around the optimum

When the maximum OSNR margin strategy described in Section III.A is used, the OSNR margin sensitivity to power variation around the optimum can be evaluated as the ratio between the OSNR margin evaluated at the optimum launched power P_{opt}^M and the OSNR margin evaluated at a launched power equal to $P_{\Delta} = \Delta \cdot P_{opt}^M$:

$$\text{Delta OSNR}_{margin} = \frac{\text{OSNR}_{margin}(P_{opt}^M)}{\text{OSNR}_{margin}(P_{\Delta})} \quad (45)$$

where:

$$\text{OSNR}_{margin}(P) = \frac{\text{OSNR}_{ASE, Rx}(P)}{\text{OSNR}_{FEC, NL}(P)} \quad (46)$$

From Eq. (30) we derive that:

$$\frac{1}{\text{OSNR}_{FEC, NL}(P_{opt}^M)} = \frac{1}{\text{OSNR}_{FEC}} - \frac{1}{\text{OSNR}_{NL}^{opt}} = \frac{2}{3} \frac{1}{\text{OSNR}_{FEC}} \quad (47)$$

Using the following relationships:

$$\text{OSNR}_{ASE, Rx}(P_{\Delta}) = \Delta \cdot \text{OSNR}_{ASE, Rx}(P_{opt}^M) \quad (48)$$

$$\text{OSNR}_{NL}(P_{\Delta}) = \frac{\text{OSNR}_{NL}(P_{opt}^M)}{\Delta^2}$$

We get:

$$\begin{aligned} \frac{1}{\text{OSNR}_{FEC, NL}(P_{\Delta})} &= \frac{1}{\text{OSNR}_{FEC}} - \frac{1}{\text{OSNR}_{NL}(P_{\Delta})} = \\ &= \frac{1}{\text{OSNR}_{FEC}} - \Delta^2 \frac{1}{\text{OSNR}_{NL}(P_{opt}^M)} = \frac{1}{\text{OSNR}_{FEC}} \left(1 - \frac{1}{3} \Delta^2 \right) \end{aligned} \quad (49)$$

and finally:

$$\begin{aligned} \text{Delta OSNR}_{margin} &= \frac{\text{OSNR}_{ASE, Rx}(P_{\Delta})}{\text{OSNR}_{FEC, NL}(P_{\Delta})} \cdot \frac{\text{OSNR}_{FEC, NL}(P_{opt}^M)}{\text{OSNR}_{FEC, NL}(P_{\Delta})} = \\ &= \Delta \left(1 - \frac{1}{3} \Delta^2 \right) \frac{3}{2} = \frac{\Delta(3 - \Delta^2)}{2} \end{aligned} \quad (50)$$

When the minimum BER strategy described in Section III.B is used, the total OSNR sensitivity to power variation around the optimum can be evaluated as the ratio between the total OSNR evaluated at the optimum launched power P_{opt}^m and the OSNR margin evaluated at a launched power equal to $P_{\Delta} = \Delta \cdot P_{opt}^m$:

$$\text{Delta OSNR}_{\text{tot}} = \frac{\text{OSNR}_{\text{tot}}(P_{opt}^m)}{\text{OSNR}_{\text{tot}}(P_{\Delta})} \quad (51)$$

where:

$$\text{OSNR}_{\text{tot}}(P) = \left(\frac{1}{\text{OSNR}_{\text{ASE,Rx}}(P)} + \frac{1}{\text{OSNR}_{\text{FEC,NL}}(P)} \right)^{-1} \quad (52)$$

From Eq. (38) we derive that:

$$\text{OSNR}_{\text{ASE,Rx}}(P_{opt}^m) = \frac{1}{2} \cdot \text{OSNR}_{\text{NL}}(P_{opt}^m) \quad (53)$$

Using Eq. (48), we get:

$$\begin{aligned} \frac{1}{\text{OSNR}_{\text{tot}}(P_{opt}^m)} &= \frac{1}{\text{OSNR}_{\text{ASE,Rx}}(P_{opt}^m)} + \frac{1}{\text{OSNR}_{\text{NL}}(P_{opt}^m)} = \frac{3}{\text{OSNR}_{\text{NL}}(P_{opt}^m)} \\ \frac{1}{\text{OSNR}_{\text{tot}}(P_{\Delta})} &= \frac{1}{\text{OSNR}_{\text{ASE,Rx}}(P_{\Delta})} + \frac{1}{\text{OSNR}_{\text{NL}}(P_{\Delta})} = \\ &= \frac{1}{\Delta \text{OSNR}_{\text{ASE,Rx}}(P_{opt}^m)} + \frac{\Delta^2}{\text{OSNR}_{\text{NL}}(P_{opt}^m)} = \\ &= \frac{1}{\Delta \frac{1}{2} \text{OSNR}_{\text{NL}}(P_{opt}^m)} + \frac{\Delta^2}{\text{OSNR}_{\text{NL}}(P_{opt}^m)} = \frac{1}{\text{OSNR}_{\text{NL}}(P_{opt}^m)} \left(\frac{2}{\Delta} + \Delta^2 \right) \end{aligned} \quad (54)$$

Finally, substituting Eq. (54) in Eq. (51), we obtain:

$$\text{Delta OSNR}_{\text{tot}} = 3 \cdot \frac{1}{\left(\frac{2}{\Delta} + \Delta^2 \right)} = \frac{3\Delta}{2 + \Delta^3} \quad (55)$$

E. Transient robustness

The goal of this section is the derivation of the analytical formulas (15) and (16) in the hypothesis of optical link with identical spans.

For a number N_d of dropped channels, let's assume that:

- the transient amplifier control is described by the parameter δ , i.e. the per-channel output power of the k-th amplifier (which, before the transient, is equal to $P_{TX,opt}$) is multiplied by a factor δ ;
- after transient, the non-linearity coefficient η is reduced by a factor χ .

Before and after the transient, the linear and non-linear OSNRs are equal to:

$$\frac{1}{\text{OSNR}_{\text{ASE,Rx}}^{\text{before}}} = \sum_1^{N_{\text{span}}} \frac{P_{\text{ASE}}}{P_{\text{TX,opt}}} = N_{\text{span}} \cdot \frac{P_{\text{ASE}}}{P_{\text{TX,opt}}}; \quad (56)$$

$$\frac{1}{\text{OSNR}_{\text{ASE,Rx}}^{\text{after}}} = \sum_{k=1}^{N_{\text{span}}} \frac{P_{\text{ASE}}}{\delta^k \cdot P_{\text{TX,opt}}} = \frac{1}{N_{\text{span}} \cdot \text{OSNR}_{\text{ASE,Rx}}^{\text{before}}} \sum_{k=1}^{N_{\text{span}}} \frac{1}{\delta^k}$$

and

$$\begin{aligned} \frac{1}{\text{OSNR}_{\text{NL}}^{\text{before}}} &= \sum_1^{N_{\text{span}}} \eta \cdot B_n \cdot (P_{\text{Tx,opt}})^2 = N_{\text{span}} \cdot \eta \cdot B_n \cdot (P_{\text{Tx,opt}})^2 \\ \frac{1}{\text{OSNR}_{\text{NL}}^{\text{after}}} &= \sum_{k=1}^{N_{\text{span}}} \chi \cdot \eta \cdot B_n \cdot (\delta^k \cdot P_{\text{Tx,opt}})^2 = \\ &= \frac{1}{N_{\text{span}} \cdot \text{OSNR}_{\text{NL}}^{\text{before}}} \chi \cdot \sum_{k=1}^{N_{\text{span}}} \delta^{2k} \end{aligned} \quad (57)$$

When the maximum OSNR margin strategy described in Section III.A is used, the OSNR margin sensitivity to the amplifier transient is given by:

$$\frac{\text{OSNR}_{\text{margin}}^{\text{after}}}{\text{OSNR}_{\text{margin}}^{\text{before}}} = \frac{\text{OSNR}_{\text{ASE,Rx}}^{\text{after}}}{\text{OSNR}_{\text{FEC,NL}}^{\text{after}}} \frac{\text{OSNR}_{\text{FEC,NL}}^{\text{opt}}}{\text{OSNR}_{\text{ASE,Rx}}^{\text{opt}}} \quad (58)$$

At the optimum,

$$\begin{cases} \frac{1}{\text{OSNR}_{\text{NL}}^{\text{opt}}} = \frac{1}{3} \frac{1}{\text{OSNR}_{\text{FEC}}^{\text{opt}}} \\ \frac{1}{\text{OSNR}_{\text{FEC,NL}}^{\text{opt}}} = \frac{2}{3} \frac{1}{\text{OSNR}_{\text{FEC}}^{\text{opt}}} \end{cases} \quad (59)$$

Furthermore, during the transient event,

$$\begin{cases} \frac{1}{\text{OSNR}_{\text{FEC,NL}}^{\text{after}}} = \frac{1}{\text{OSNR}_{\text{FEC}}^{\text{opt}}} - \frac{1}{\text{OSNR}_{\text{NL}}^{\text{after}}} \\ \frac{1}{\text{OSNR}_{\text{ASE,Rx}}^{\text{after}}} = \frac{1}{N_s \cdot \text{OSNR}_{\text{ASE,Rx}}^{\text{opt}}} \sum_{k=1}^{N_{\text{span}}} \frac{1}{\delta^k} \\ \frac{1}{\text{OSNR}_{\text{NL}}^{\text{after}}} = \frac{1}{N_s \cdot \text{OSNR}_{\text{NL}}^{\text{opt}}} \chi \cdot \sum_{k=1}^{N_{\text{span}}} \delta^{2k} \end{cases} \quad (60)$$

Substituting Eq. (59) in Eq. (60):

$$\begin{aligned} \frac{1}{\text{OSNR}_{\text{FEC,NL}}^{\text{after}}} &= \frac{1}{\text{OSNR}_{\text{FEC}}^{\text{opt}}} - \frac{1}{N_s \cdot \text{OSNR}_{\text{NL}}^{\text{opt}}} \chi \cdot \sum_{k=1}^{N_{\text{span}}} \delta^{2k} \\ &= \frac{1}{\text{OSNR}_{\text{FEC}}^{\text{opt}}} - \frac{1}{3} \frac{1}{N_s \cdot \text{OSNR}_{\text{FEC}}^{\text{opt}}} \chi \cdot \sum_{k=1}^{N_{\text{span}}} \delta^{2k} \end{aligned} \quad (61)$$

Replacing Eqs. (61) and (59) in Eq. (58):

$$\frac{\text{OSNR}_{\text{margin}}^{\text{after}}}{\text{OSNR}_{\text{margin}}^{\text{before}}} = \frac{3}{2} \left(1 - \frac{1}{3 \cdot N_{\text{span}}} \chi \sum_{k=1}^{N_{\text{span}}} \delta^{2k} \right) \frac{N_{\text{span}}}{\sum_{k=1}^{N_{\text{span}}} \frac{1}{\delta^k}} \quad (62)$$

Finally, using the following relationship from geometric series properties:

$$\sum_{k=1}^N x^k = \frac{x - x^{N+1}}{1 - x} \quad (63)$$

we get:

$$\frac{\text{OSNR}_{\text{margin}}^{\text{after}}}{\text{OSNR}_{\text{margin}}^{\text{before}}} = \frac{3}{2} \left(N_{\text{span}} - \frac{\chi}{3} \left(\frac{\delta^2 - \delta^{2N_{\text{span}}+2}}{1 - \delta^2} \right) \right) \frac{1 - \frac{1}{\delta}}{\frac{1}{\delta} - \frac{1}{\delta^{N_{\text{span}}+1}}} \quad (64)$$

Similarly, when the minimum BER strategy described in Section III.B is used, the sensitivity of the total OSNR to amplifier transient can be derived. Before and after the transient:

$$\begin{aligned}
\frac{1}{\text{OSNR}_{\text{tot}}^{\text{before}}} &= \frac{1}{\text{OSNR}_{\text{tot}}^{\text{opt}}} = \frac{1}{\text{OSNR}_{\text{ASE,Rx}}^{\text{opt}}} + \frac{1}{\text{OSNR}_{\text{NL}}^{\text{opt}}} \\
\frac{1}{\text{OSNR}_{\text{tot}}^{\text{after}}} &= \frac{1}{\text{OSNR}_{\text{ASE,Rx}}^{\text{after}}} + \frac{1}{\text{OSNR}_{\text{NL}}^{\text{after}}} = \\
&= \frac{1}{N_{\text{span}} \cdot \text{OSNR}_{\text{ASE,Rx}}^{\text{opt}}} \sum_{k=1}^{N_{\text{span}}} \frac{1}{\delta^k} + \frac{1}{N_{\text{span}} \cdot \text{OSNR}_{\text{NL}}^{\text{opt}}} \chi \cdot \sum_{k=1}^{N_{\text{span}}} \delta^{2k}
\end{aligned} \tag{65}$$

Taking into account that, at the optimum for minimum BER, $\text{OSNR}_{\text{NL}}^{\text{opt}} = 2 \cdot \text{OSNR}_{\text{ASE,Rx}}^{\text{opt}}$, and using Eq. (63), the following expression can be derived from Eq. (65) for the sensitivity of the total OSNR to the amplifier transient:

$$\frac{\text{OSNR}_{\text{tot}}^{\text{after}}}{\text{OSNR}_{\text{tot}}^{\text{before}}} = \frac{3}{2} N_{\text{span}} \left(\frac{\frac{1}{\delta} - \left(\frac{1}{\delta}\right)^{N_{\text{span}}+1}}{1 - \frac{1}{\delta}} + \frac{\chi}{2} \cdot \frac{\delta^2 - (\delta^2)^{N_{\text{span}}+1}}{1 - \delta^2} \right)^{-1} \tag{66}$$

REFERENCES

- [1] O. Gerstel, M. Jinno, A. Lord, and S. Yoo, "Elastic optical networking: a new dawn for the optical layer?" *IEEE Commun. Mag.*, vol. 50, no. 2, pp. s12–s20, Feb. 2012.
- [2] P. Poggiolini, "The GN Model of non-linear propagation in uncompensated coherent optical systems" *J. of Lightw. Technol.*, vol. 30, no. 24, pp. 3857-3879 (2012).
- [3] R. Pastorelli, G. Bosco, A. Nespola, S. Piciaccia, F. Forghieri, "Network Planning Strategies for Next-Generation Flexible Optical Networks," in Proc. OFC 2014, paper M2B.1, San Francisco (USA), Mar. 2014.
- [4] E. Grellier and A. Bononi, "Quality parameter for coherent transmissions with Gaussian-distributed nonlinear noise," *Opt. Exp.*, nol. 19, no. 13, pp. 12781-12788 (2011).
- [5] Xi Chen and W. Shieh, "Closed-form expressions for nonlinear transmission performance of densely spaced coherent optical OFDM systems," *Opt. Exp.*, vol. 18, no. 18, pp. 19039-19054 (2010).
- [6] M. Secondini, E. Forestieri, E., "Analytical Fiber-Optic Channel Model in the Presence of Cross-Phase Modulation," *IEEE Photon. Technol. Lett.*, vol. 24, no. 22, pp. 2016-2019, Nov. 15, 2012.
- [7] M. Nazarathy et al., "Phased-array cancellation of nonlinear FWM in coherent OFDM dispersive multi-span links," *Opt. Exp.*, vol. 16, no. 20, pp.15777-15810 (2008).
- [8] P. Poggiolini et al., "The LOGON Strategy for Low-Complexity Control Plane Implementation in New-Generation Flexible Networks", in Proc. OFC 2013, paper OW1H.3, Anaheim (USA), Mar. 2013.
- [9] K. Roberts and C. Laperle, "Flexible Transceivers," in Proc. ECOC 2012, paper We.3.A.3, Amsterdam, Sep. 2012.
- [10] R. Pastorelli, et al., "Optical Control Plane Based on an Analytical Model of Non-Linear Transmission Effects in a Self-Optimized Network," in Proc. ECOC 2013, paper We.3.E.4, London (UK), Sep. 2013.
- [11] A. Nespola et al., "Extensive Fiber Comparison and GN-model Validation in Uncompensated Links using DAC-generated Nyquist-WDM PM-16QAM Channels," in Proc. OFC 2013, paper OTh3G.5, Anaheim (USA), Mar. 2013.
- [12] G. Bosco, A. Carena, R. Cigliutti, V. Curri, P. Poggiolini, F. Forghieri, "Performance prediction for WDM PM-QPSK transmission over uncompensated links," in Proc. OFC 2011, paper OTh07, Los Angeles (USA), Mar. 2013.